ELSEVIER

Journal of Molecular Liquids 84 (2000) 17–27

journal of MOLECULAR LIQUIDS

www.elsevier.nl/locate/molliq

Molecular dynamics simulation and EPR spectroscopy of nitroxide side chains in bacteriorhodopsin

Heinz-Jürgen Steinhoff[a], Matthias Müller[a], Christian Beier[a] and Matthias Pfeiffer[b]

[a]Lehrstuhl für Biophysik, Ruhr-Universität Bochum, 44780 Bochum, Germany
[b]Max-Planck-Institut für Biochemie, Am Klopferspitz 18 a, 82152 Martinsried, Germany

A novel approach for the simulation of electron paramagnetic resonance (EPR) spectra was used to combine molecular dynamics (MD) simulations with experimental data. Reorientational dynamics trajectories of a sequence of nitroxide side chains attached to cysteine substitution mutants of bacteriorhodopsin (BR) were calculated by means of MD simulations. EPR spectra calculated from these data were found to be in excellent agreement with the experimental spectra. Simulation of EPR difference spectra for two BR conformations reveal that experimentally detected changes of the nitroxide dynamics during the catalytic cycle of BR are consistent with a transient conformational change of helix F.

1. INTRODUCTION

The investigation of protein motions and related conformational changes is a prerequisite for the understanding of enzymatic processes. The development of suitable techniques which provide high spatial and high time resolution is a major challenge for biophysical research. In the present approach, electron paramagnetic resonance (EPR) spectroscopy is combined with molecular dynamics (MD) simulations to study the dynamics of a sequence of nitroxide side chains introduced into the light driven proton pump bacteriorhodopsin (BR). Photo activation of the intrinsic chromophore retinal initiates a catalytic cycle which is accompanied by a transient structural change of BR. The side chain motions of nitroxides attached to positions 165 through 171 and the modulation of their dynamics during the catalytic cycle is subject of the present study.

The continuous wave (cw) EPR spectral line shape of a spin labeled protein depends on the nitroxide side chain mobility and thus allows us to characterize the protein dynamics in a wide correlation time range from picoseconds to nanoseconds; The application of saturation transfer spectroscopy extends the time range to milliseconds [1-3]. Site directed mutagenesis has allowed to introduce nitroxide side chains at almost any desired site in a protein (for reviews see, e.g., [4, 5]). Recent studies on a large number of spin labeled mutants of BR and lysozyme have shown that the dynamic properties of the nitroxide side chain and thus the EPR spectral line shape contain indeed direct information about the secondary and tertiary structure of the protein in the vicinity of the nitroxide binding site [6, 7]. The application to rhodopsin and BR, e.g., revealed structural data of certain protein domains, which could not be resolved with other techniques [8, 9]. Time resolved analysis of the nitroxide dynamics of a whole set of spin labeled proteins allows the characterization of structural changes during protein function. Recently, conformational changes of colicin E and lysozyme were studied during

0167-7322/00/$ - see front matter
PII S0167-7322(99) 00107-5

their function [10, 11], and structural changes of rhodopsin and BR were monitored after photo activation [8, 12, 13].

However, a quantitative interpretation of these experimental data in terms of motional mechanisms, fluctuation amplitudes and correlation times requires the simulation of EPR spectra. Simulations on the basis of dynamic models [14-16] show excellent agreement with the corresponding experimental spectra of solvated spin labels or spin-labeled lipids and give valuable insight in the dynamics of these systems. However, the dynamics of a protein bound spin label is extremely complex, involving interaction of the nitroxide with the protein backbone, adjacent side chains and collisions with solvent molecules. Recently, a method was developed, which allows simulations of EPR spectra of nitroxides on the basis of MD simulations [17]. This approach offers the advantage to study the influences of the structure of the spin label binding site on the EPR spectral line shape with atomic resolution. In a first application of this method we present here studies of the dynamics of nitroxide side chains at positions 165 to 171 in the cytoplasmic moiety of helix F of BR. This part of helix F is found to perform a reversible outward movement during the catalytic cycle of BR [18]. The corresponding changes of the side chain dynamics are investigated by the combined methods of EPR spectroscopy and MD simulations.

2. METHODS

2.1. Sample preparation and EPR spectroscopy

Site-directed mutagenesis and spin labeling was performed as described by Pfeiffer et al. [9]. EPR spectra were recorded with a home made X-band EPR spectrometer equipped with a Bruker dielectric resonator. The BR samples (5 µl) were loaded into EPR quartz capillaries at a final concentration of 200 µM. Spectra were taken at 293 K at a microwave power of 1 mW and a modulation amplitude of 1.5 G. After analog to 12 bit digital conversion, the data were processed in a personal computer.

2.2. Molecular dynamics simulations

The atomic coordinates of BR were taken from the Brookhaven Protein Data Bank [19]. The nitroxide side chain of the spin label (1-oxyl-2,2,5,5-tetramethylpyrroline-3-methyl) methanethiosulfonate (MTSSL), Figure 1, was attached to the respective cysteines. Reorientation trajectories of the bound nitroxides were calculated from stochastic dynamics (SD) or molecular dynamics (MD) simulations by means of the GROMOS program library (Biomos, Groningen). Aliphatic CH, CH2, and CH3 groups, as well as aromatic CH groups were treated as extended carbon atoms. Bond lengths and positions of the backbone atoms were constraint using the SHAKE algorithm [20]. Since we were interested only in the spatial restrictions of the nitroxide motion Coulomb interactions were excluded from the calculations. After energy minimization, the backbone atoms were fixed and the system was equilibrated at 50 K, then heated up to 300 K and finally to 600 K. This temperature was chosen to guarantee that the total space accessible for the reorientation of the nitroxide is covered within reasonable computation time. SD simulations with total lengths of 2 ns were performed using a friction coefficient of 4 ps^{-1}, MD simulations were performed for up to 4 ns. The time step of the integration of the equations of motion were set to 2 fs. All calculations were done with an Alpha Station 600 5/266 (Digital). The orientation history of

the z-axis of the nitroxide ring is expressed in terms of Euler angles α, β and γ, with respect to the initial orientation of the ring plane.

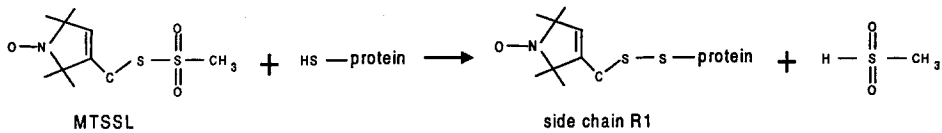

Figure 1. Structure of the spin label MTSSL and its reaction with the protein to yield the nitroxide side chain R1.

2.3. EPR spectra calculations from the nitroxide reorientation trajectories

Here we present a short overview of the techniques applied; a detailed description of the simulation methodology is given by Steinhoff and Hubbell [17]. The direct calculation of EPR spectra from the results of a MD simulation requires the length of the trajectory to be larger than the transverse relaxation time, T_2, which is of the order of 100 ns. Since MD simulations on proteins can only be performed up to several nanoseconds within a reasonable computation time, the problem has to be reduced. For this purpose MD trajectories of the spin labeled protein with a total length of up to 4 ns were used to calculate potentials of mean force which represent the interaction of the nitroxide with neighboring side chains and the protein backbone. In a second step, the nitroxide is represented by a single particle which is subject to these potentials of mean force. The effect of the solvent and of the fluctuation of the neighboring side chains is represented by a random fluctuating force. Trajectories of the nitroxide reorientation $\Omega(t)$ with lengths of 700 ns were then derived from the numerical solution of the Langevin equation for rotational diffusion.

Due to the anisotropy of the g- and the hyperfine coupling tensors, the Lamor frequency of the unpaired electron located in the pi orbital of the nitroxide depends on its molecular orientation with respect to the magnetic field. The time course of the Lamor frequency, $\omega(t)$ is determined from the eigenvalues of the spin Hamiltonian, $H(\Omega(t))$. The trajectory of the complex magnetization, M(t), is subsequently calculated from $\omega(t)$ by solving the Bloch equations numerically [21]. The observed dispersion and absorption EPR signals follow from the real and imaginary parts of the Fourier transform of an ensemble average of M(t).

3. RESULTS AND DISCUSSION

3.1. Experimental analysis of the nitroxide dynamics

To introduce a nitroxide side chain into helix F of BR, residues 165 to 171 were mutated to cysteines one by one and subsequently modified with the sulfhydryl-specific reagent MTSSL to give the nitroxide side chain R1 (see Figure 1) [9]. Figure 2 shows the structure of the BR backbone together with various modified residues. The side chains R1 at positions 165 and 169 are located on the outer surface of helix F close to the lipid-water interface and face either the aqueous (165) or the lipid phase (169). The side chains at positions 166 and

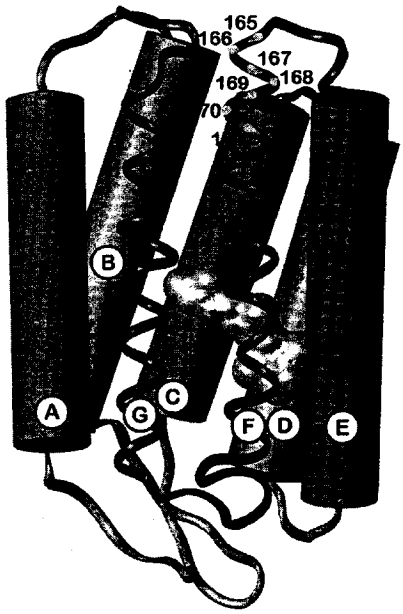

Figure 2. The backbone structure of BR. The seven transmembrane helices, which are denoted A through G, surround the chromophore retinal (shown space filled). The natural amino acids from positions 165 to 171 in the cytoplasmic domain of helix F were exchanged by cysteines one by one.

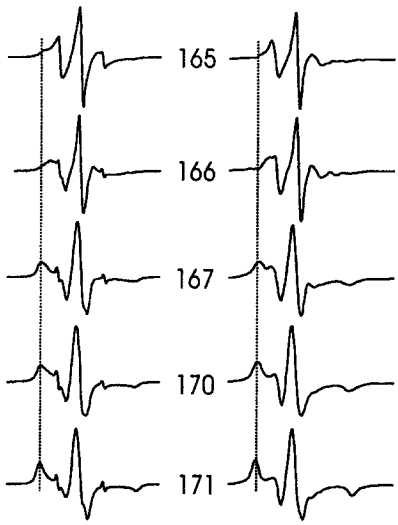

Figure 3. *Left column:* Experimental EPR spectra of BR mutants spin labeled at positions 165 through 171. The vertical line indicates the position of the low field hyperfine extreme that characterizes immobilized nitroxides. *Right column:* EPR spectral simulations based on MD trajectories. The effective potentials were calculated from the angle populations, examples of which are shown in Figure 5.

170 are oriented towards helix G and those attached to positions 167 and 171 point towards helix C into the proton uptake channel. The nitroxide at position 168 is oriented towards helix E.

The shape of the EPR spectra reflect the degree of reorientational motion of the nitroxide side chain. This residual motion results from rotational isomerizations about internal bonds of the side chain and depends on the secondary and tertiary structure in the vicinity of the spin label binding site. Weak interaction between the nitroxide and the rest of the protein results in a high degree of mobility. In this case, the apparent hyperfine splitting and the line width are small as found for the spectra of P165R1 and E166R1 (Figure 3). In turn, if the residual motion is restricted due to strong interaction of the nitroxide group with neighboring side chains or backbone atoms, the apparent hyperfine splitting and the line width are increased. This is obvious for the spectra V167R1, T170R1 and F171R1.

In spite of the complicated nature of the nitroxide dynamics (see below) simple parameters extracted from the spectra were found to be correlated with the secondary structure of the binding site environment. Thus, Hubbell and coworkers have shown that the variation of the line widths of the center lines, ΔH, or of the second moment, $\langle H^2 \rangle$, of the complete spectra yield information on the secondary structure, if a complete set of spin labeled mutants is studied [5]. The variation of the line width together with measurements of the accessibility of the nitroxides for paramagnetic quenchers were used, e.g., to propose a structural model of the E-F loop of BR [9]. The square root of the second moment, $\langle H^2 \rangle^{1/2}$, can be shown to be linearly related to the apparent hyperfine splitting. This apparent hyperfine splitting is in turn related to the mean square fluctuation angle $\langle \Delta\beta^2 \rangle$ of the nitroxide pi orbital [22, 23]. For small fluctuation angles and rapid fluctuations the relation between $\langle H^2 \rangle^{1/2}$ and $\langle \Delta\beta^2 \rangle$ can be shown to be linear. Therefore, in the present approach, $\langle H^2 \rangle^{1/2}$, is taken as parameter to characterize the nitroxide dynamics. The experimental values determined for the spectra shown in Figure 3 and of two additional spectra (A168R1 and S169R1) published by Pfeiffer et al. [9] are depicted as a function of the sequence position in Figure 4. The helical character of the cytoplasmic moiety of helix F is reflected by the oscillation of $\langle H^2 \rangle^{1/2}$. Relative minima are found at positions 165 and 169, high values of $\langle H^2 \rangle^{1/2}$ are revealed for side chains at positions 168 and 171. This finding agrees with the structural data of BR, which show the side chains of P165 and S169 being located at the outside of helix F, whereas those of A168 and F171 are buried inside the protein.

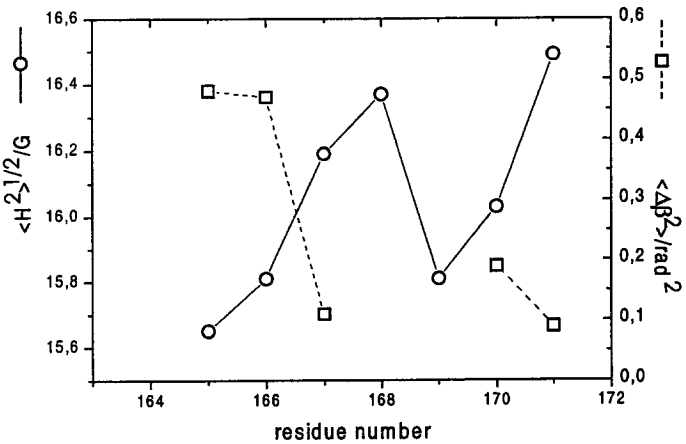

Figure 4. As a measure of the nitroxide side chain dynamics the square root of the second moment, $\langle H^2 \rangle^{1/2}$, was calculated from the experimental spectra shown in Figure 3 and depicted as a function of the residue number (circles). The oscillation of $\langle H^2 \rangle^{1/2}$ reflects directly the secondary structure of the F helix in the studied region. The mean square fluctuation of the nitroxide ring calculated from MD trajectories (squares) is in reverse phase to $\langle H^2 \rangle^{1/2}$.

3.2. MD simulations of the nitroxide dynamics

Orientation trajectories of the nitroxide z axes with respect to a space fixed coordinate system are shown in Figure 5 for three selected residues, P165R1, V167R1 and T170R1. These residues were selected to discuss the major properties of the side chain dynamics. The orientation of the z axis of the nitroxide attached to position 165 at the outer surface of helix F covers nearly the entire angle space (Figure 5a). The population density of orientations reveals a sine ß weighting similar to what is expected for an isotropic orientation distribution. The interaction energy for reorientational motion of the nitroxide consists of torsion terms and a small number of nonbonded interactions of the atoms of the nitroxide side chain and the fixed protein backbone. This interaction leaves wide ranges of orientations with low energy. In contrast, the population densities for the nitroxide orientations for V167R1 and T170R1 clearly show well defined extremes (Figure 5b, c). The nitroxide of V167R1 occupies a highly populated orientation with ß = 3 rad. A lower and very broad extreme is found near ß = 0.7 rad. Within these local potential minima, the nitroxide ring performs fast librational oscillations of small amplitude. The reorientation between the two major orientations appears to be a jump diffusion like process. The nitroxide attached to position 170 is buried inside the protein. Due to steric restrictions only fast reorientational oscillations

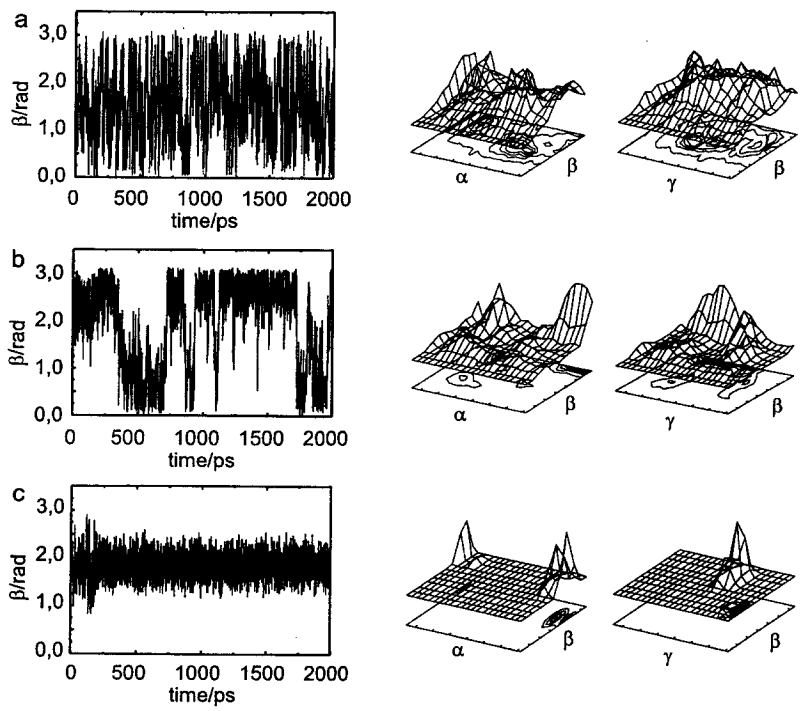

Figure 5. Reorientation angle β motion of the nitroxide z axis for three spin label side chains at position 165 (a), 167 (b) and 170 (c). The angle population densities calculated from these trajectories are shown on the right as a function of the Euler angles α, β and γ. α and γ range from -π to +π, β from 0 to π.

of the nitroxide ring of small amplitude are observable. The angle population plots reveal a highly anisotropic reorientational motion of the attached nitroxides at positions 167 and 170.

In conclusion, the motion of the spin label side chain consists of two major types of fluctuations. On a short time scale (1 ps), angle fluctuations with rms fluctuation angle $<\Delta\beta^2>^{1/2}$ of 0.06-0.1 rad are found that represent oscillations within discrete potential minima. On a longer time scale, jumps between these potential valleys occur with orientation changes of large amplitude (> 0.5 rad). From simulations at 300 K a correlation time of 1.5 ns was estimated for a helix-bound nitroxide in an aqueous environment [17]. A similar behavior has been reported for the reorientation of a spin label bound to methemoglobin and for the dihedral angle fluctuations of side chains in lysozyme [23, 24].

3.3 Combining EPR experiment and MD simulation

For a first comparison of the MD results with experimental data, the mean square fluctuation amplitude $<\Delta\beta^2>$ is calculated from the trajectories. The values are shown in Figure 4 as a function of the residue position. The fluctuation amplitude varies with the residue position and clearly reflects the helical character of the spin labeled moiety of helix F. The inverse correlation of $<\Delta\beta^2>$ to the experimental parameter $<H^2>^{1/2}$ is obvious. This result may be regarded as a first prove of a successful combination of MD simulations and EPR experiments. We conclude that the square root of the second moment of experimental EPR spectra is a direct measure of the accessible motion cone of the nitroxide.

However, the central goal in the combination of MD simulations and EPR experiments is to account for the complex character of the nitroxide dynamics. Thus, the simulation of the EPR spectra and a detailed comparison with experimental data should give valuable information of the protein structure in the nitroxide vicinity, the side chain dynamics and possible conformational changes. Steinhoff and Hubbell [17] have shown that a Hamiltonian could be found that allows EPR spectra to be calculated from MD simulation trajectories of the considered spin labels. A comparison of EPR spectra simulated in that way with calculations using Freed´s program [14, 15] for isotropic Brownian diffusion shows that the approach chosen yields EPR spectra with the correct splitting, line shape and transverse relaxation times. It was also demonstrated, that this method can be applied to protein bound nitroxides [17]. Here, we present an application of this approach to the nitroxides side chains at positions 165, 166, 167, 170 and 171. Single particle trajectories were calculated from the numerical solution of the Langevin equation with free energy surfaces taken from the population densities (cf. Figure 5 for the samples P165R1, V167R1 and T170R1). Magnetization trajectories were calculated from 200 trajectories for 100 different sine ß weighted orientations of the BR molecule as described [17]. The rotational diffusion coefficient was set to 0.05 ns^{-1} corresponding to an isotropic rotational correlation time of 3 ns to account for frictional effects of side chains and solvent. The g-tensor and hyperfine values chosen are: $g_{xx} = 2.0090$, $g_{yy} = 2.0065$, $g_{zz} = 2.0025$, $A_{xx} = A_{yy} = 5$ G, $A_{zz} = 35$ G. To account for additional inhomogeneous line broadening the magnetization trajectories were multiplied by $\exp(-t/T_2)$, with $T_2 = 30$ ns for P165R1 and E166R1, and $T_2 = 20$ ns for the other samples. The Fourier transform of the average of the resulting 20000 magnetization trajectories yield the desired EPR absorption spectra (Figure 3). The comparison with the experimental data in Figure 3 reveals agreement of the spectral shape and splitting for the whole sequence shown. The increase of the motional restrictions due to tertiary interaction is visible in the appearance of outer peaks in the low field and high field extremes of both the

simulated and the experimental spectra (indicated by vertical bars). It should be stressed that the diffusion coefficient is held constant for the total set of samples. The agreement between simulation and experiment demonstrates that the spectral shape is mainly determined by the spatial restriction of the nitroxide motion. The influence of a possible variations of the local viscosity on the line shape plays a minor role. Moreover, our results indicate that the structural data obtained for BR under highly unphysiological conditions seem to hold also under physiological conditions, i.e. in the native membrane. This seems to be true at least for the cytoplasmic end of helix F.

3.4. Conformational changes alter the nitroxide side chain dynamics at position 171

Photon absorption by the all-trans retinal initiates a cyclic series of transformations with discrete intermediates, designated K through O, which are identified by their optical absorbance maxima and kinetic properties. This catalytic cycle of BR results in a net proton translocation across the membrane. Transient conformational changes of BR during the photocycle were revealed by X-ray, neutron and electron diffraction experiments [18, 25-27]. Time resolved Fourier transform infrared spectroscopy has identified structural changes in the protein backbone during the M to N transition [28]. However, the mechanism and the characteristics of the structural changes are still obscure. Diffraction experiments yield data about the location of the conformational changes, which indicate a reordering of helix G and an outward tilt of helix F. These experiments, however, suffer from limited time resolution. Time resolved EPR studies of spin labeled cysteine mutants revealed transient changes of the nitroxide side chain dynamics located in the C-D loop and in the E-F loop [12, 13, 29]. In the following section we show that the combination of MD simulations with EPR spectra calculation will help to understand the site dependent pattern of transient mobilization and immobilization of the nitroxide during a conformational change. For this purpose we studied the EPR spectral change of the spin label side chain at position 171 during the photocycle.

Changes of the EPR spectral shape were monitored during a magnetic field scan by phase sensitive detection referenced to the triggering source of a light shutter [12]. This detection scheme leads to the difference EPR spectrum between the excited and the initial state conformations. The resulting difference spectrum observed for F171R1 is shown in Figure 6a. The changes of the spectral amplitudes at the low field and high field extremes are

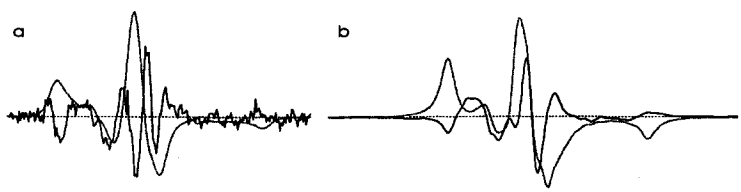

Figure 6. (a) Experimental EPR difference spectra of the spin label side chain F171R1 detected during the photocycle of BR. The full line shows the difference of the spectrum of intermediate N minus that of the initial state. The absorption spectrum of the initial state is shown by the dashed line. (b) Simulated difference spectra of F171R1 for the two F helix conformations shown in Figure 7. The dashed line shows the simulated spectrum of the initial conformation.

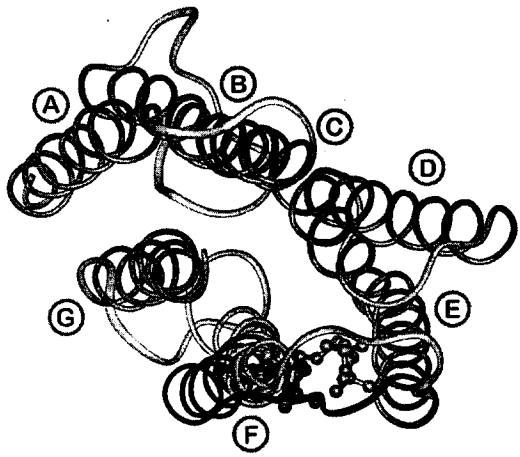

Figure 7. View onto the cytoplasmic surface of the BR backbone. The helices are denoted A through F. A spin label is attached to helix F at position 171. Two conformations are shown which differ in the tilt of the cytoplasmic part of helix F (light and black) resulting in different locations of the spin label side chain.

evidence for an increase of the nitroxide mobility. For example, the transient reduction of the peak amplitude of the low field maximum is accompanied by a transient lowering of the low field minimum. This behavior is expected when the motional freedom of the nitroxide is increased. Very similar difference spectra with reversed polarity were recorded for nitroxides attached at positions 101 and 103 [12, 29], which both were transiently immobilized during the photocycle.

As outlined above, we again combine EPR experiments with MD simulations. Whereas an atomic model of high resolution is available for BR in the initial state [19, 30], the structural changes occurring during the photocycle are only known on a very low resolution level. Neutron [25] and X-ray [26] experiments have shown that the most intense difference peak in the M minus BR difference map is a positive peak at the position of helix G. Additionally, electron crystallography uncovered a prominent positive/negative pair of peaks located at the position of helix F [18, 27]. The authors interpret these changes as an outward tilting of the cytoplasmic half of helix F. Our aim is to show that such a tilt fits our experimental data determined for the nitroxide at position 171. For an approximation of the atomic data of the kinked helix F we took the atomic coordinates of the BR fragment 163 to 231 which were determined by NMR spectroscopy [31]. A comparison of the fragment with the atomic data of native BR [19] revealed agreement in the extracellular moiety of the molecule. At the cytoplasmic end of helix F, however, an outward tilt by 5.2 angstrom was visible (structural data set No 7 given in [31]). Figure 7 depicts a superposition of these helix fragments with the spin label attached to position 171. Since the direction of the tilt and its amplitude coincide with data expected from the M minus BR difference maps shown by Subramaniam and coworkers [18], we take these data as a model of the transient structure occurring during the M to N transition of the BR photocycle. From this model we conclude that the distance of the spin label binding site and the adjacent helix E is increased during this conformational change, thus leading to an increase of the motional freedom of the nitroxide. This is indeed consistent with our experimental observations.

We performed MD simulations of the reorientational dynamics of the nitroxide at position 171 of the tilted helix and compared the results with those determined for the native BR structure. The mean square fluctuation amplitude of the spin label motion increased from 0.07 rad^2 for the BR state to 0.42 rad^2 for the modified helix structure. EPR spectra were calculated from the nitroxide reorientation transients for both structures. The result of the spectral difference shown in Figure 6b reveals a remarkable agreement with the experimental data of Figure 6a. The difference amplitudes in the low and high field region which are indicative for the increase of the motional freedom are clearly reproduced by the simulation. Therefore, a tilt of helix F agrees very well with our experimental data. However, further EPR experiments and simulation studies that probe the cytoplasmic half of BR are necessary to complete this picture [32].

4. CONCLUSION

Here, we present a first application of a new methodology which combines EPR spectroscopy and MD simulations. The results show that EPR spectra calculations based on MD simulations of protein bound spin labels are feasible within reasonable expense of computation time. The analysis confirms that the EPR spectral shape of MTSSL is determined by the spatial restrictions of the reorientational dynamics of the nitroxide side chain. Effects due to a possible variation of the local viscosity are found to be negligible. The spatial restrictions depend in a characteristic way on the secondary and tertiary structure in the spin label binding site environment. This dependence allows this method to be used, e.g., for structural refinement of low resolution data. MD simulations show that the EPR spectral changes detected during the photocycle of BR are in agreement with a transient outward tilt of helix F. Using site directed spin labeling and the respective molecular dynamic simulations high resolution models of the conformational changes of proteins during their function should be achievable.

ACKNOWLEDGMENT

We gratefully acknowledge the support of the Deutsche Forschungsgemeinschaft SFB 394, C1 (H.-J. S.) and SFB 533, A4 (M. P.).

REFERENCES

1. L. J. Berliner (ed.), Spin Labeling I, Theory and Application. Academic Press Inc., New York, 1976.
2. L. J. Berliner (ed.), Spin Labeling II, Theory and Application. Academic Press Inc., New York, 1979.
3. L. J. Berliner and J. Reuben (eds.), Biological Magnetic Resonance 8, Spin Labeling, Plenum Press, New York, 1989.
4. W. L. Hubbell and C. Altenbach. Current opinions in Struct. Biology 4 (1994) 566.
5. W. L. Hubbell, H. S. Mchaourab, C. Altenbach, and M. A. Lietzow. Structure 4 (1996) 779.
6. C. Altenbach, T. Marti, H. G. Khorana, and W. L. Hubbell. 1990. Science 248 (1990) 1088.

7. H. S. Mchaourab, M. A. Lietzow, K. Hideg, and W. L. Hubbell. Biochemistry 35 (1996) 7692.
8. C. Altenbach, K. Yang, D .L. Farrens, Z. T. Farahbakhsh, H. G. Khorana and W. L. Hubbell. Biochemistry 35 (1996) 12470.
9. M. Pfeiffer, T. Rink, K. Gerwert, D. Oesterhelt and H.-J. Steinhoff. J. Mol. Biol. (1998) submitted.
10. Y. Shin, C. Levinthal, F. Levinthal and W. L. Hubbell. Science 259 (1993) 960.
11. H. S. Mchaourab, K. J. Oh, C. J. Fang and W. L. Hubbell. Biochemistry 36 (1997) 307.
12. H.-J. Steinhoff, R. Mollaaghababa, C. Altenbach, K. Hideg, M. Krebs, H. G. Khorana, and W. L. Hubbell. Science 266 (1994) 105.
13. T. Rink, J. Riesle, D. Oesterhelt, K. Gerwert, and H.-J. Steinhoff. Biophys. J. 73 (1997) 983.
14. J. H. Freed, in: Spin Labeling Theory and Applications (Berliner, L.J., ed.) pp 53-132, Academic Press, New York 1976.
15. D. J. Schneider and J. H. Freed in: Biological Magnetic Resonance 8, Spin Labeling (L. J. Berliner and J. Reuben, eds), pp 1, Plenum Press, New York, 1989.
16. M. Ge and J. Freed. Biophys. J. 65 (1993) 2106.
17. H.-J. Steinhoff and W. L. Hubbell. Biophys. J. 71 (1996) 2201.
18. S. Subramanian, M. Gerstein, D. Oesterhelt, and R. Henderson. EMBO J. 12 (1993) 1.
19. N. Grigorieff, T. A. Ceska, K. H. Downing, J. M. Baldwin and R. Henderson. J. Mol. Biol. 259 (1996) 393.
20. W. F. van Gunsteren and H. J. C. Berendsen. Mol. Phys. 45 (1982) 637.
21. B. H. Robinson, L. J. Slutsky, and F.P. Auteri. J. Chem. Phys. 96 (1992) 2609.
22. S. P. Van, G. b. Birrell and O. H. Griffith. J. Magn. Reson. 15 (1974) 444.
23. H.-J. Steinhoff and C. Karim. Ber. Bunsenges. Phys. Chem. 97 (1993) 163.
24. C. M. Dobson and M. Karplus, in: Methods in Enzymology 131, (C. H. Hirs and S. N. Timasheff, eds.), pp. 362, Academic, New York 1986.
25. N. Dencher, G. Dresselhaus, G. Zaccai, and G. Büldt. Proc. Natl. Acad. Sci. USA. 86 (1989) 7876.
26. M. H. J. Koch, N. A. Dencher, D. Oesterhelt, H.-J. Plön, G. Rapp, and G. Büldt. EMBO J. 10 (1991) 521.
27. F. M. Hendrickson, F. Burkard and R. M. Glaeser. Biophys. J. 75 (1998) 1446.
28. G. Souvignier and K. Gerwert. Biophys. J. 63 (1992) 1393.
29. R. Mollaaghababa, H.-J. Steinhoff, W. L. Hubbell and G. H. Khorana. (1998) submitted.
30. L. O. Essen, R. Siegert, W. D. Lehmann and D. Oesterhelt. Proc. Natl. Acad. Sci. USA 95 (1998) 11673.
31. I. L. Barsukov, D. E. Nolde, A. L. Lomize and A. S. Arseniev. Eur. J. Biochem. 106 (1992) 665.
32. T. Rink, M. Pfeiffer, K. Gerwert, D. Oesterhelt, and H. -J. Steinhoff. (1998) submitted.